IONIZATION OF NOBLE GAS ATOMS BY ^{252}Cf FISSION FRAGMENTS

BY

BUNKER MILLER HILL

DEPARTMENT OF PHYSICS

University Undergraduate Fellow, 1990-91

Texas A&M University

APPROVED:

Fellows Advisor

Honors Program Director

TABLE OF CONTENTS

I. INTRODUCTION

As an energetic ion passes through matter, it interacts with the electrons and nuclei in its path. The strength of the interaction and its resulting effect depend upon the charge, relative velocity and distance of closest approach of the projectile ion and its collision partner. At low energies, where ion velocities are comparable to the velocities of the valence electrons of the atoms, ions will undergo elastic collisions with other nuclei. At high velocities, comparable to inner shell electronic velocities, the projectile may begin picking up electrons from the inner shells of the atoms. At considerably higher velocities, the outer electrons of atoms are essentially pushed out of their orbits by the electric impulse of the passing ion. The interactions of the medium with high velocity ions, addressed in the present work, are predominantly electronic in nature, and usually result in ion production. Ions produced by collisions are referred to as recoil-ions. One way of expressing the probability for the single and multiple ionization of atoms in ion-atom collisions is in the form of a cross-section. This number is expressed in cm^2 and is a very important parameter for characterizing ion production and the interactions involved.[1]

The objectives of this project are to (a) design and build a time-of-flight spectrometer system to investigate heavy-ion collisions with neutral atoms using ^{252}Cf fission fragments as a source of the heavy-ions (b) optimize the system to obtain the best resolution and efficiency possible, (c) obtain charge state distributions and

ionization cross sections for ^{252}Cf fission fragments and alpha particles in collision with the noble gases (excluding Radon), and (d) compare the charge state distributions and ionization cross sections for the above collisions with theoretical predictions and the results of previous heavy-ion collision work.[2,3,4,5,6,7]

The primary purpose of this work was to study the charge state distributions and ionization cross sections for fast, highly charged, heavy ions in collision with noble gas atoms. Fission fragments from the spontaneous fission of the isotope ^{252}Cf provide a simple way of extending ionization cross section and charge state distribution measurements for ion-atom collisions in the 0.5 to 1.0 MeV/amu energy region to much higher projectile atomic numbers and ionic charges than are available at most particle accelerators. In addition, a spontaneous fission source is much less expensive than a particle accelerator and can be dedicated to an individual experiment for large amounts of time. It is expected that the system developed for the present study will be useful in future experiments involving dissociative, multielectron ionization of molecules, since large amounts of time are required to collect data. The investigation of collisions between ^{252}Cf fission fragments and single atoms in the gas phase may eventually lead to new insights regarding the complex processes involved in plasma desorption mass spectrometry.

II. BACKGROUND

A. Previous Work

The effectiveness of energetic heavy-ion collisions in producing highly charged, low energy recoil ions was first demonstrated by Cocke[2] in 1979. Using time-of-flight spectroscopy Cocke was able to identify Ar ions with charges up to 11+ in collisions of 28 to 43 MeV Cl^{6-13+} beams with gaseous Ar. He found that the ionization cross-sections varied only slightly with energy but quite drastically with projectile charge.[7] Maurer[7] also was able to see Ar^{11+} in time-of-flight experiments employing 40 MeV Ar^{13+} projectiles.

B. Theory

There are two main processes by which a target atom may be ionized by a fast, highly charged projectile. One process is known as pure, or direct, ionization. This ionization occurs as a result of the Coulomb interaction of the projectile with the electrons of the target atom. The cross section for direct ionization is theoretically predicted to vary as the square of the projectile charge. Direct ionization is thought to be the primary process leading to the production of target recoil-ions having low-charges ($q < 4+$) in ion-atom collisions at high velocities.[1] The second process is electron capture. Electron capture, as the name implies, occurs when the projectile captures electrons from the target atom. This ionization process occurs predominantly when the projectile velocity approaches the velocity of the orbiting electrons in

the neutral target atom.[1] For the fast velocity regime addressed in the present experiments, this velocity matching condition is fulfilled only for inner-shell electrons, and therefore it is expected that electron capture will only be of importance in small impact parameter collisions. It is likely that electron capture plays a dominant role in the production of recoil ions having high charges ($q > 4+$).[8]

C. Nuclear Properties of Californium-252

The heavy isotope of ^{252}Cf is formed by intense neutron irradiation of Bk. The nucleus of ^{252}Cf is composed of 98 protons and 154 neutrons. It is unstable and undergoes both alpha decay (96.9%) and spontaneous fission (3.1%) with a half life of 2.64 years. Through alpha decay, a ^{252}Cf nucleus emits a 6.1 MeV alpha particle and forms an excited daughter nucleus of ^{248}Cm. As a result of spontaneous fission, the ^{252}Cf nucleus splits into two unequal parts.[9] Schematically, the two branches of the ^{252}Cf decay process are shown in figure 1.

In fact, the fission decay does not always produce the same two fragments but rather two distinct distributions of fragments. The heavy fragment distribution is centered about ^{142}Cs while the light fragment distribution is centered about ^{106}Tc. The heavy and light fragments typically have energies of approximately 78 MeV and 104 MeV, respectively.[9] An energy spectrum of the ^{252}Cf decay products, measured with a Si surface barrier detector, is shown in figure 2.

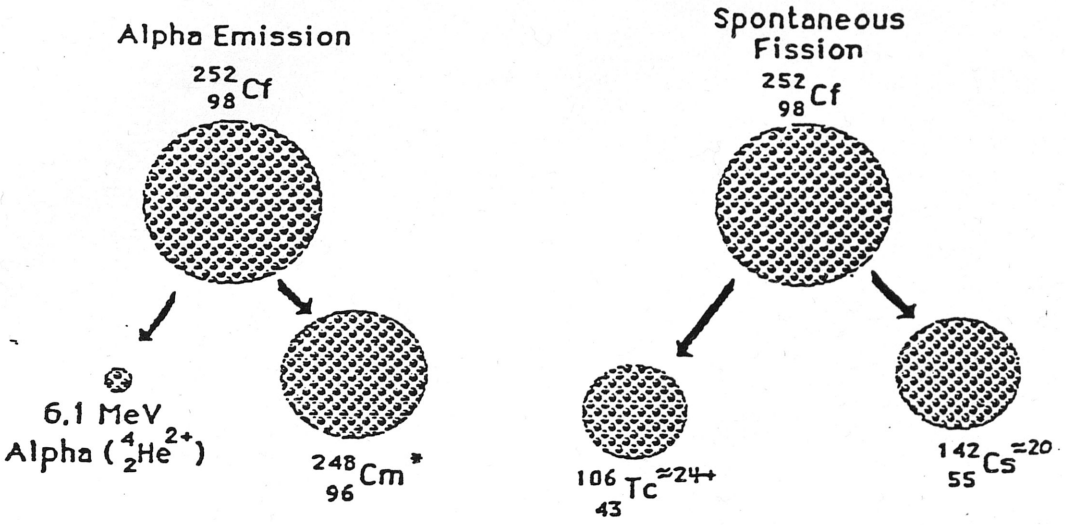

Figure 1. Schematic representation of a) alpha decay and b) spontaneous fission of ^{252}Cf.

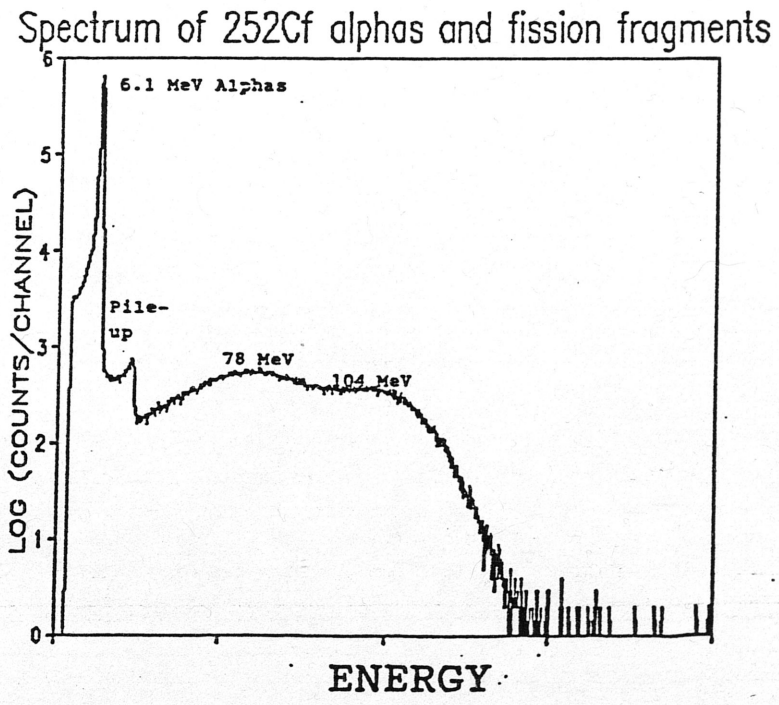

Figure 2. Pulse-height energy spectrum of ^{252}Cf obtained using a Si surface barrier detector. The 6.1 MeV alpha peak, the alpha pile-up peak, and the heavy and light fission fragment distributions are seen.

The nominal activity of the ^{252}Cf source used in the present experiments was 25 μCi. The source consisted of a 4mm spot of Cf_2O_3 electroplated onto a 50 $\mu g/cm^2$ layer of Au attached to a 1 mg/cm^2 Ni foil and covered with another identically constructed Au/Ni foil combination. Alpha particles emitted from the decaying ^{252}Cf within the source lost approximately 0.4 MeV in passing through the Au/Ni foil combination. The heavy and light fission fragments emerged from the foil with 48 MeV and 73 MeV, respectively. At this energy, the equilibrium charge states of the heavy and light fission fragment distributions are estimated to be +19.5 and +20.5, respectively. These equilibrium charges are the averages of the charges calculated using the semi-empirical prescriptions of Sayer, Baron, Baudinet-Robinet, Nikolaev-Dimitriev, and Shima.

III. EXPERIMENTAL METHODS

A. Time-of-flight Method

Time-of-flight spectrometry is a proven technique for studying recoil ions. The method is based on the principle that the time of flight of an ion that has been accelerated through an electric field is directly proportional to the square root of its mass to charge ratio. This fact is easily derived from simple classical mechanics. The acceleration of a charged particle in an electric field is

$$a = qE/m, \qquad (1)$$

where q is the ionic charge, E the electric field strength, and m the

mass of the ion. The distance traveled under that acceleration, assuming static starting conditions, is

$$d = at^2/2. \qquad (2)$$

For a given distance traveled in an electric field, the time of flight is

$$t = (2d/a)^{1/2}, \qquad (3)$$

which becomes

$$t = [2dm/(qE)]^{1/2} \qquad (4)$$

when equation (1) is substituted for the acceleration in equation (3). Factoring out the known constants into a single constant, K, and assuming a constant electric field, one obtains

$$t = K(m/q)^{1/2}. \qquad (5)$$

Therefore, each characteristic mass to charge ratio gives a unique time of flight.

Typically electrode separations in time of flight systems are on the order of one centimeter. The dimensions are kept small so that the electric field remains uniform. In addition, the electric field is usually quite large (hundreds of volts per centimeter) so that high ion extraction efficiency is achieved. From the above equations we see that a small d combined with a high E gives a small flight time. Small flight times correspond to small separations between the flight times of

ions having different mass to charge ratios, and thus to poor resolving power. In order to remedy this situation, a field free region may be added to the flight path of the ions. The velocity of ions that enter the field free flight tube is determined by the kinetic energy, E_k, which they gained in passing through the electric field, as shown below.

$$E_k = qEd = mv^2/2, \qquad (6)$$

where

$$v = (2qEd/m)^{1/2} \qquad (7)$$

The time it takes the ion to travel the field free distance, d', is simply

$$t = d'/v = d'[m/(2qEd)]^{1/2}, \qquad (8)$$

which is still directly proportional to the square root of the mass to charge ratio, but is also directly proportional to the field free distance, d'. Therefore, a longer flight tube gives better time separation for different mass to charge ratios, and therefore better resolution.

B. Spectrometer System

The time-of-flight spectrometer used for the present work is shown in Figure 3. It differed from other time-of-flight spectrometers used in experiments at the Texas A&M University Cyclotron Institute in that it was designed to accommodate a ^{252}Cf fission source and a Si Surface Barrier Detector (SBD). The spectrometer was also constructed so that it could be mounted on a flange

and easily removed from the high vacuum chamber. The cylindrically symmetric spectrometer was composed of a gas cell, a ^{252}Cf fission source, an Si SBD, a top electrode, a collimator, a field-free flight tube, and a recoil-ion microchannel plate detector. The cell consisted of a 17.0 mm. inner diameter Cu cylinder covered by a heavy Ni screen. The gas entered through the screen and the gas pressure was monitored by means of a capacitance manometer which was connected to another feedthrough at this location. The cylinder had a hole of 3.23 mm. diameter for the fission fragments to enter, and a coaxial hole of 4.06 mm. for the fission fragments to exit on the opposite wall. The ^{252}Cf was mounted flush against the cylinder and maintained at the same voltage as the Cu cylinder so as to perturb the field as little as possible. An 88% transmission Ni grid covered the fission fragment exit hole to reduce possible electric field perturbations. The brass conical collimator was maintained at a lower potential than the top electrode and cell walls. This created a uniform electric field in the gas cell and a slightly focusing second stage accelerating field between the collimator and the grid covering the flight tube. The equi-potential lines for the spectrometer system, as calculated using the electrostatic lens program SIMION[10], are shown in figure 4. The gas cell, top electrode, collimator, Si SBD, and ^{252}Cf source were all held in a fixed geometry by a non-conducting nylon housing.

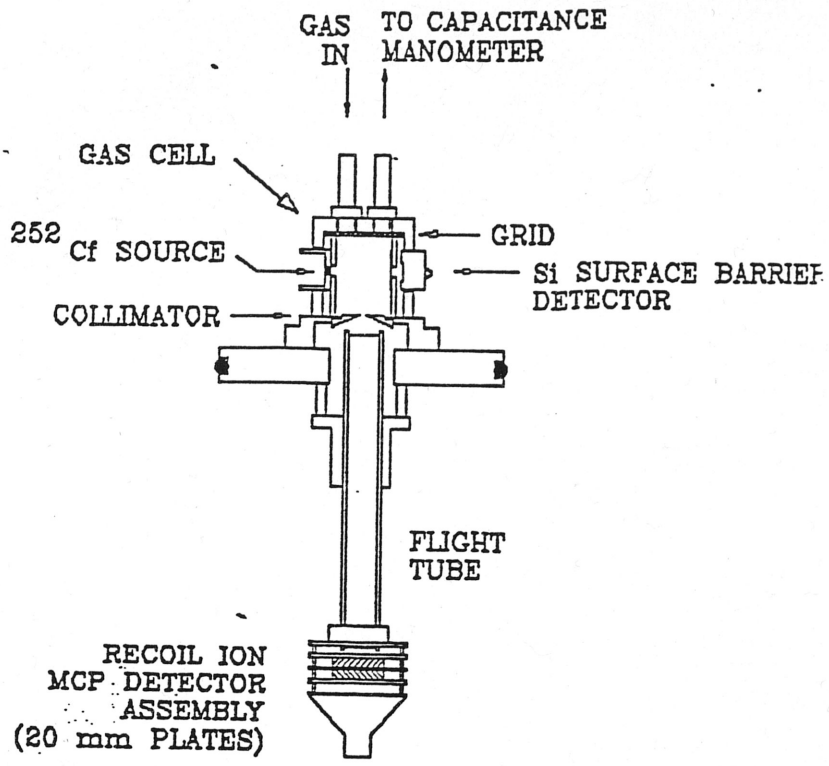

Figure 3. Diagram showing the gas cell, ^{252}Cf source, fission fragment detector, and TOF spectrometer arrangement.

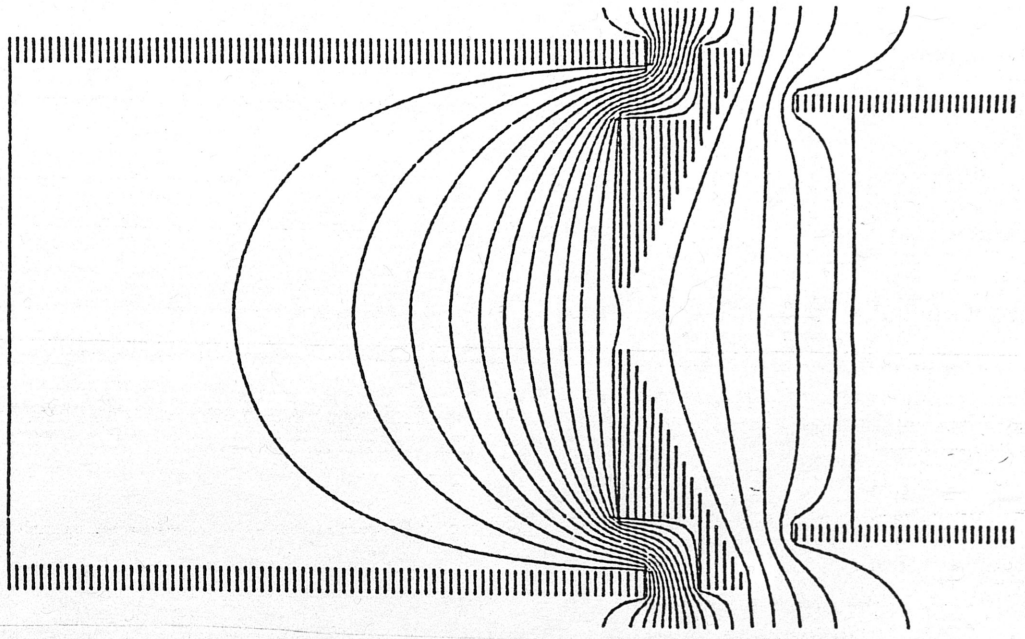

Figure 4. SIMION plot of the equi-potential lines within the TOF spectrometer.

The fission fragments from the ^{252}Cf source entered the cell, traveled through the interaction region, and then struck the Si SBD. The SBD provided a start signal for determining the time of flight. Recoil ions produced by collisions of projectile ions with target gas atoms were extracted from the cell by the electric field. If an ionization occurred close enough to the spectrometer axis, the ion passed through the collimator hole and was accelerated and focused into the flight tube by the second acceleration stage. The ion then drifted through the flight tube and upon exiting was accelerated into a microchannel plate detector system (MCP) to provide a stop signal for the time-of-flight determination.

The interaction region within the gas cell was defined by the collimator, fission fragment entrance hole, and fission fragment exit hole. Only ion trajectories which fell within a cylinder defined by the collimator's 2.74 mm hole could reach the MCP system. The fission fragments from the ^{252}Cf source were emitted into the majority of the gas cell volume. However, start signals could be generated only for fission fragments that hit the SBD. Therefore only the narrow conical beam of fission fragments defined by the entrance and exit holes was utilized in the experiment. The intersection of the conical fission fragment beam and the cylindrical collimator defined the interaction region. The two dimensional projection of this region (perpendicular to both the fission fragment and collimator axis) had the shape of an isosceles trapezoid and was very close to being rectangular.

The best resolution of the spectrometer is achieved when all of the recoil ions are produced at exactly the same position within the gas cell. Since this is not the case in the present experiments, as discussed above, the resolution of the spectrometer would appear to depend upon the difference in flight times of identical ions produced at the extreme limits of the interaction region. However, a two stage time-of-flight spectrometer is capable of what is known as space focusing which, in principle, enables ions produced at various distances above and below the beam axis to arrive at the MCP detector at the same time. It was shown by Wiley and McLaren[11] that one unique value of the voltage ratio V_1/V_2 (V_1 is the voltage difference between the top electrode and the collimator, and V_2 is the voltage difference between the collimator and the entrance to the flight tube) will satisfy the space focusing condition. The optimum values of V_1 and V_2 were experimentally determined by adjusting the ratio until the best resolution was obtained. The optimum voltages were found to be V_1 = +1250 V and V_2 = +400 V. The best resolution obtained (determined by the FWHM of the time peak) was approximately 8 nanoseconds for Ar^{1+}.

C. Vacuum System

The time-of-flight spectrometer required a high vacuum to minimize secondary collisions and for proper detector operation. At the same time, a relatively high target gas pressure was needed to obtain a reasonable counting rate. These conflicting demands required that a differential pumping system be designed and implemented. A schematic

diagram of the differentially pumped gas cell and vacuum system is shown in Figure 5.

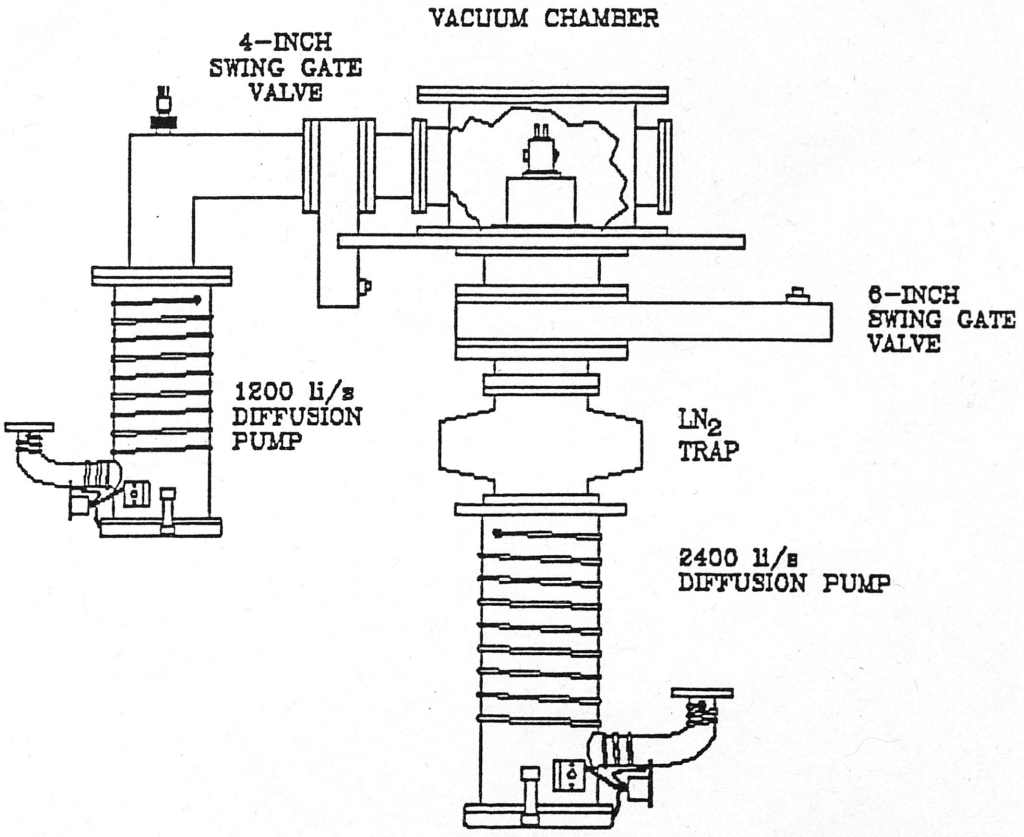

Figure 5. Schematic diagram of the differentially pumped gas cell and vacuum system.

A 6-inch diffusion pump (2400l/s) connected to a cold trap and mounted to the bottom of the 12-inch diameter stainless steel vacuum chamber, pumped directly on the gas cell. The pressure in the gas cell (nominally 1 mTorr) was regulated by means of a needle valve and a capacitance manometer. The valve and manometer were mounted outside of the chamber and connected to the top of the gas cell by about 10 inches

of .25 inch I.D. Tygon tubing. Another diffusion pump (4-inch) was mounted on an arm of the main chamber. It kept the main chamber and region where the Si SBD was located at a pressure below 8×10^{-6} Torr when gas was flowing through the cell. This pressure was monitored by an ionization gauge connected to one of the chamber's 6 flanges. The electronic system was connected to the spectrometer by means of high vacuum BNC to BNC feed-throughs in one of the flanges on the main chamber.

D. Electronic System

A schematic representation of the electronics system is shown in Figure 6. Fast timing signals from the SBD preamplifier were sent to a constant fraction discriminator (CFD) and used to generate start signals for a time-to-amplitude converter (TAC). Signals from the MCP detector were sent through a fast amplifier to a CFD and used to generate stop signals for the TAC. The time differences between the start and stop signals were the times of flight of ions produced in fission fragment collisions. These time difference signals were converted into a time spectrum by means of an IBM PC with a NUCLEUS multi-channel analyzer card (PCA).

The time-of-flight scale was calibrated using a TAC calibrator. The TAC calibrator sent timed pulses of a known periodicity to the TAC. This produced periodic time peaks in the PCA spectrum from which the slope and intercept of the linear relationship between time and channel number were determined.

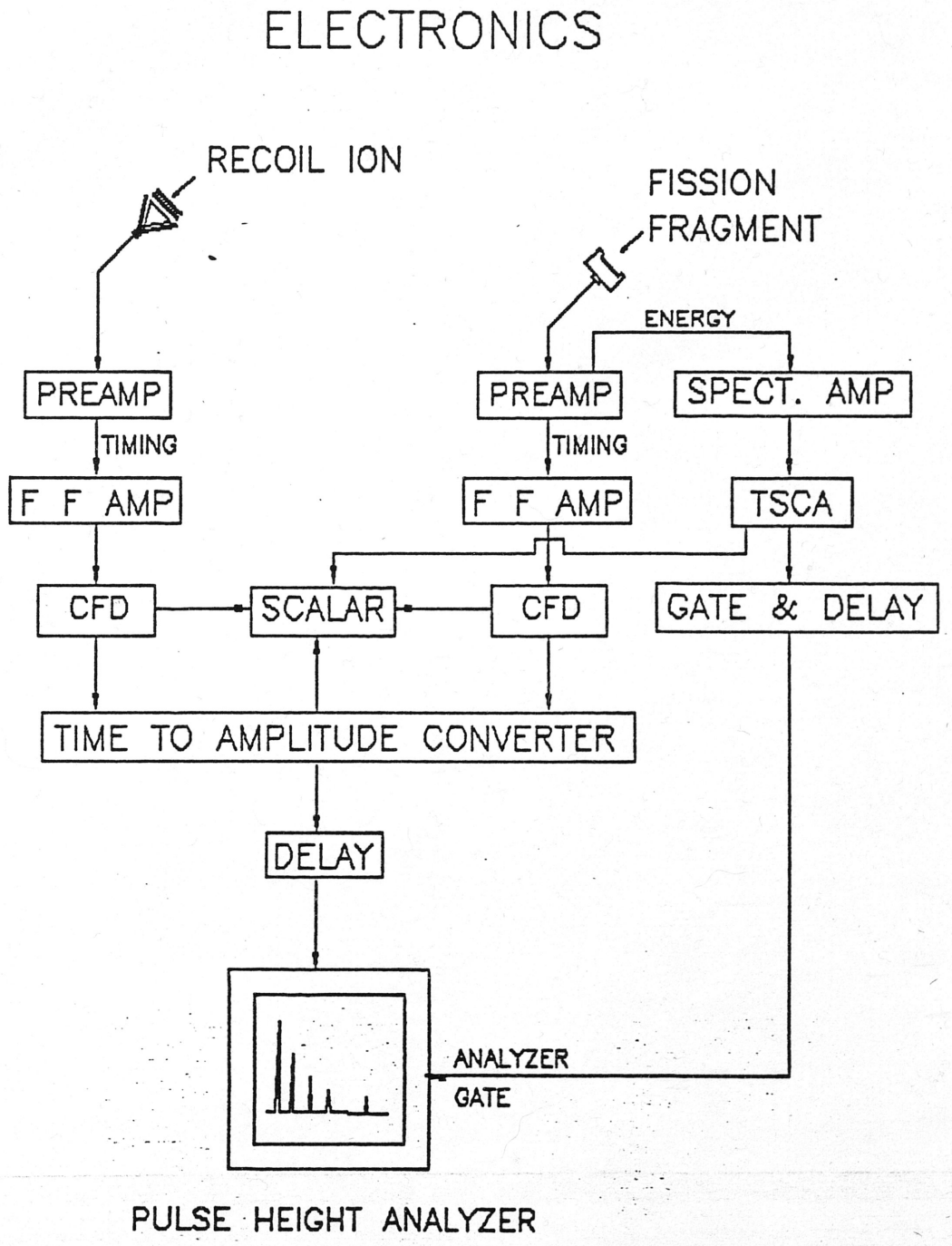

Figure 6. Schematic representation of the electronics system used to both select projectile energy and obtain time-of-flight spectra.

Energy signals from the SBD preamplifier were sent through a linear amplifier and from there to a timing single channel analyzer (TSCA). The TSCA was used to select the energy/mass range of the projectiles by placing a window around the signals of interest. In this way, either the heavy fragment peak or the light fragment peak could be chosen. Since ^{252}Cf is also an intense source of 6.1 MeV alpha particles, ionization cross sections for alpha particles could be measured by selecting the alpha peak. The output signals from the TSCA were used to gate the PCA so that only TAC signals for which the TSCA window requirement was fulfilled were recorded in the time spectrum. In addition, the TSCA also provided a fast negative timing pulse for each gate signal it generated. This signal was sent to a scalar so that the total number of detected projectiles within the selected energy range of the TSCA could be counted.

IV. DATA ANALYSIS AND RESULTS

Following voltage optimization, time calibration, and modification of the spectrometer design (final version shown previously in Figure 3) data acquisition began. In separate measurements, the 6.1 MeV alpha particles and the ^{252}Cf fission fragments were used as the ionizing projectiles. Each measurement lasted from 12 to 48 hours. The energy range of accepted projectiles, the total number of projectiles, the gas pressure, and the time spectrum (number of counts versus time of flight) were recorded for each measurement.

The mass to charge ratio could be determined from each time peak, and thus the specific charge state of the recoil-ion could be identified. In addition, peaks due to residual gases (O_2, N_2, H_2O, for example) could also be identified in the spectra. Typical time-of-flight spectra for He, Ne, Ar, Kr, and Xe ions produced by 6.1 MeV alpha particle impact are shown in figures 7-11. Time-of-flight spectra for the same ions produced by ^{252}Cf fission fragment collisions are shown in figures 12-16.

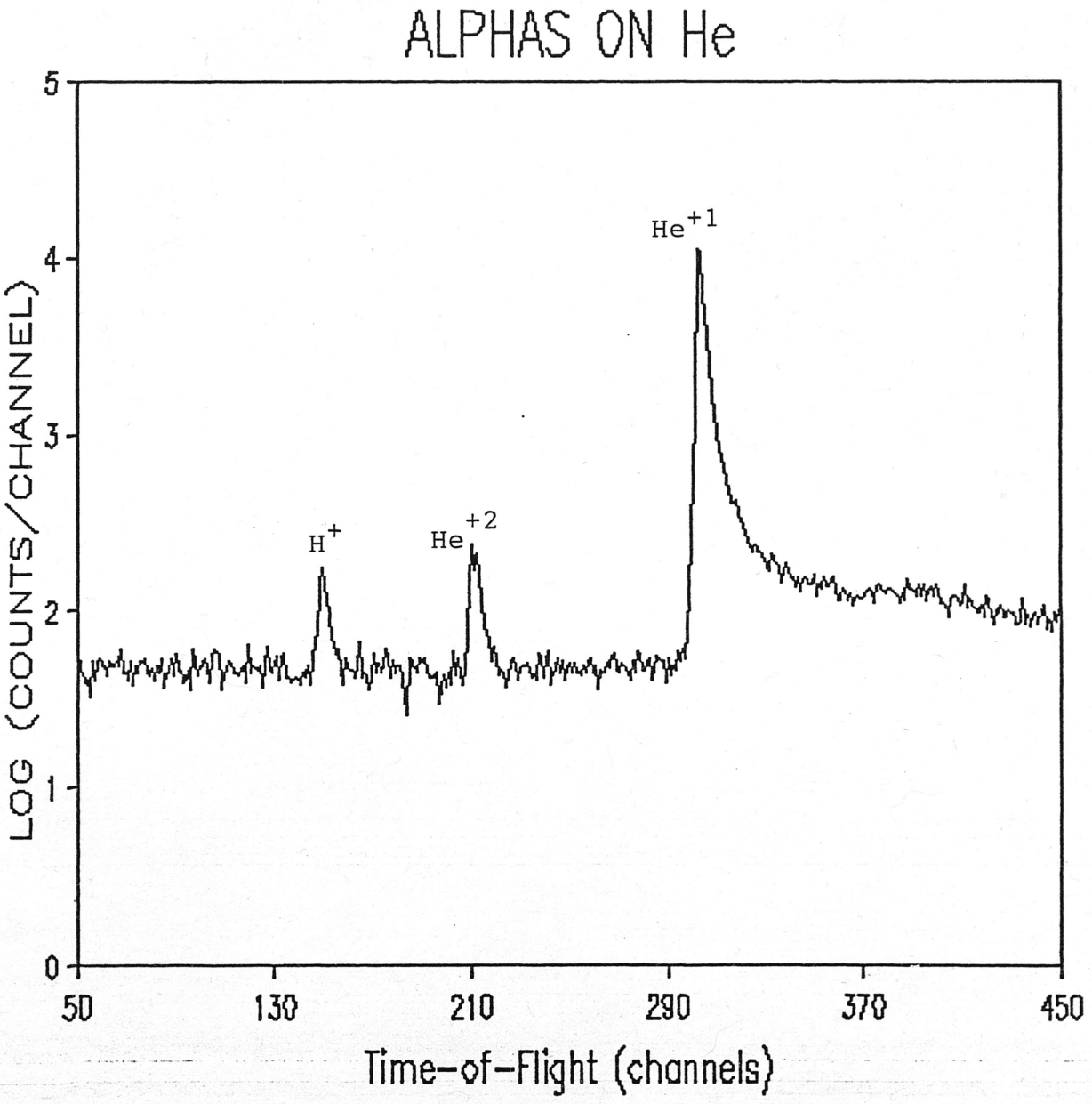

Figure 7. TOF spectrum of He recoil ions produced by collisions of 5.7 MeV alpha particles with He.

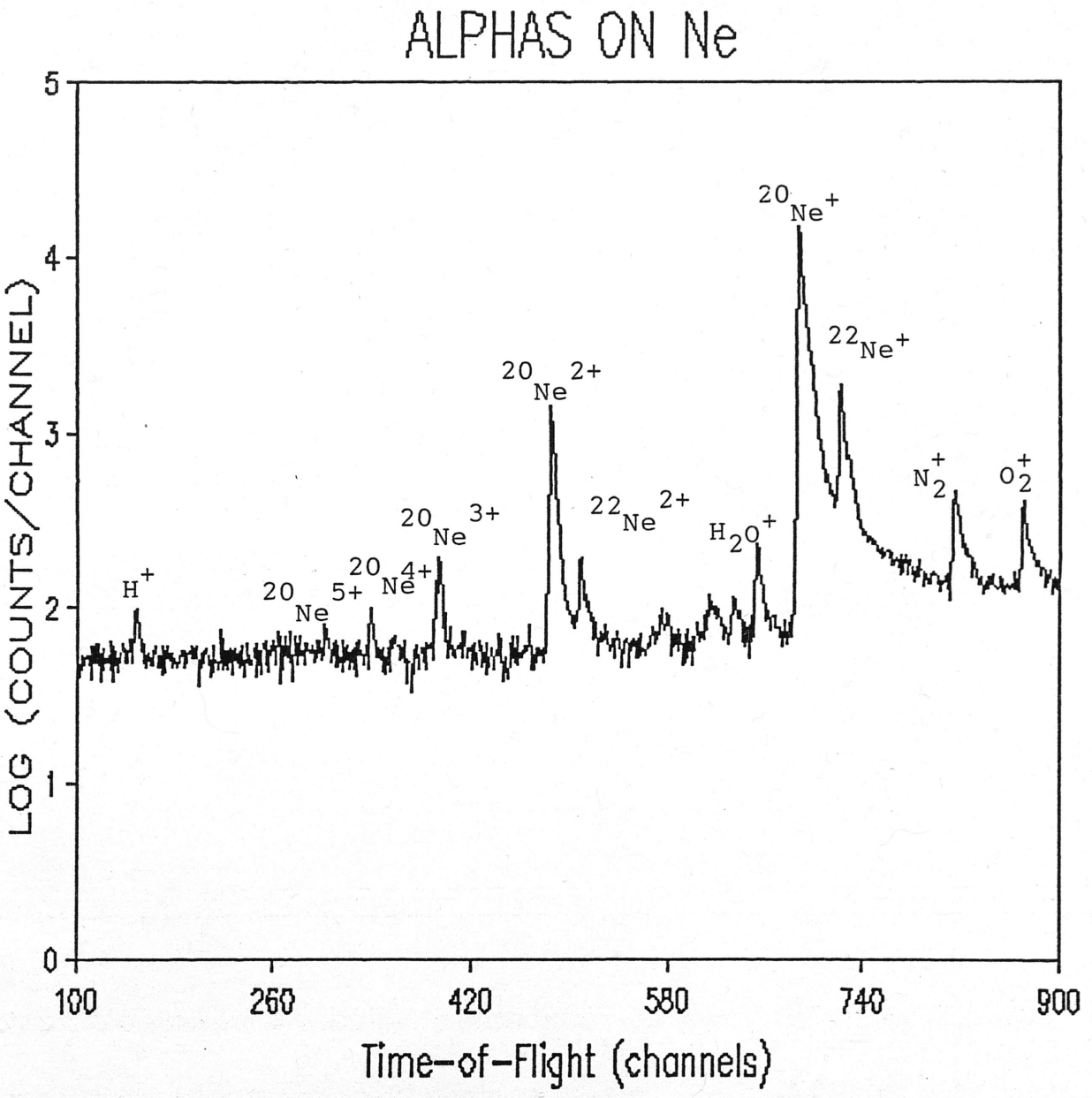

Figure 8. TOF spectrum of Ne recoil ions produced by collisions of 5.7 MeV alpha particles with Ne.

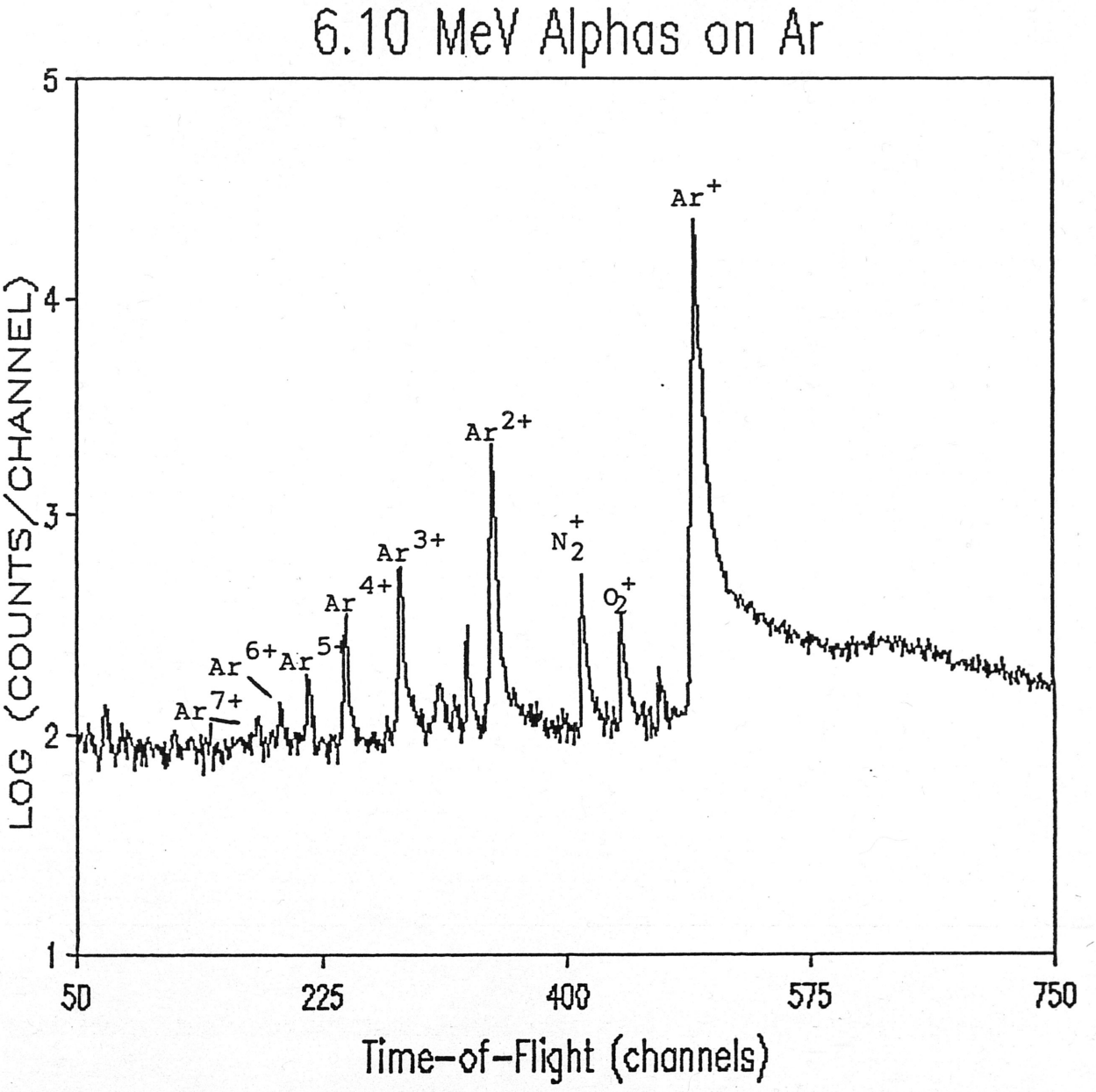

Figure 9. TOF spectrum of Ar recoil ions produced by collisions of 5.7 MeV alpha particles with Ar.

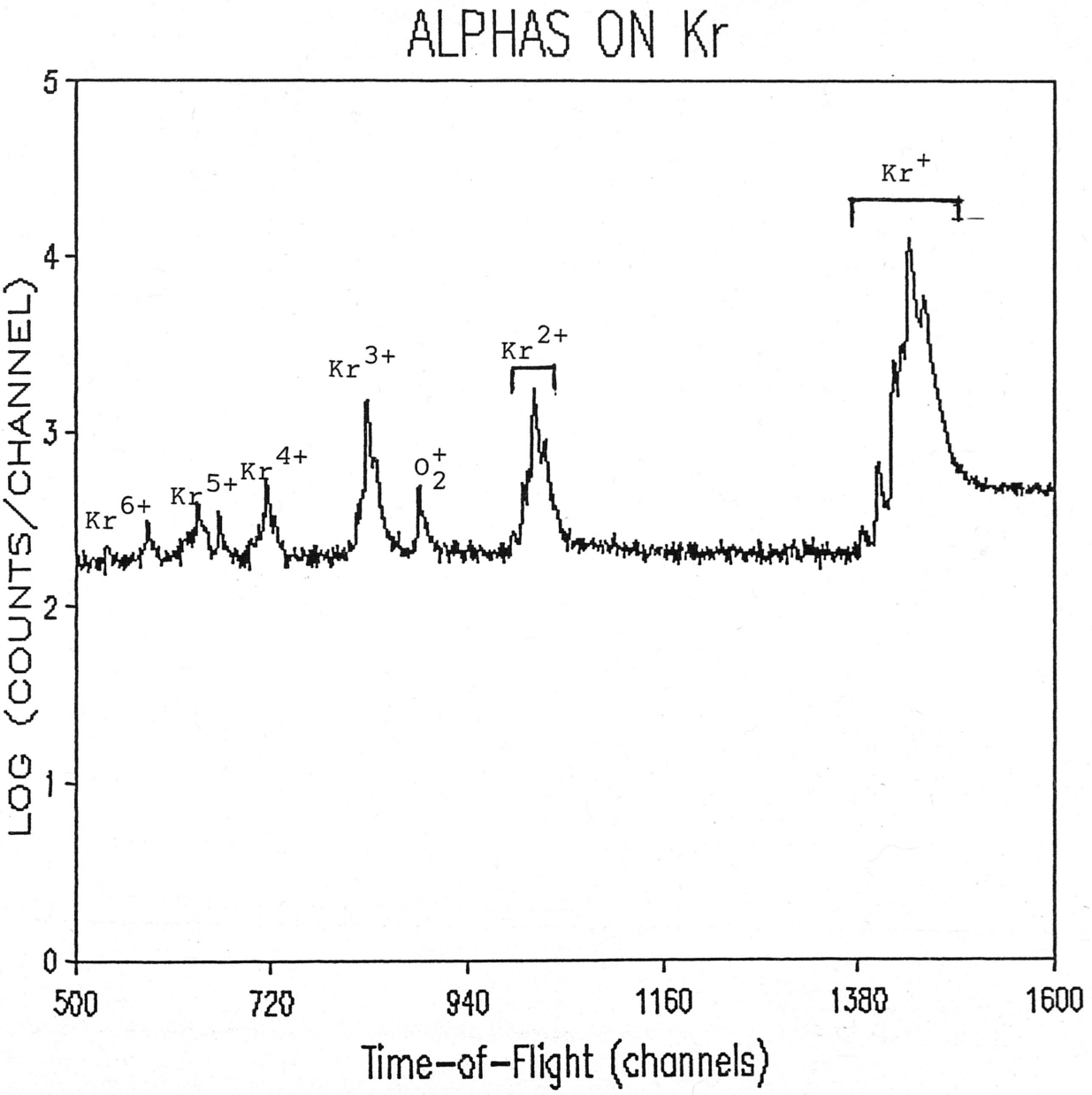

Figure 10. TOF spectrum of Kr recoil ions produced by collisions of 5.7 MeV alpha particles with Kr.

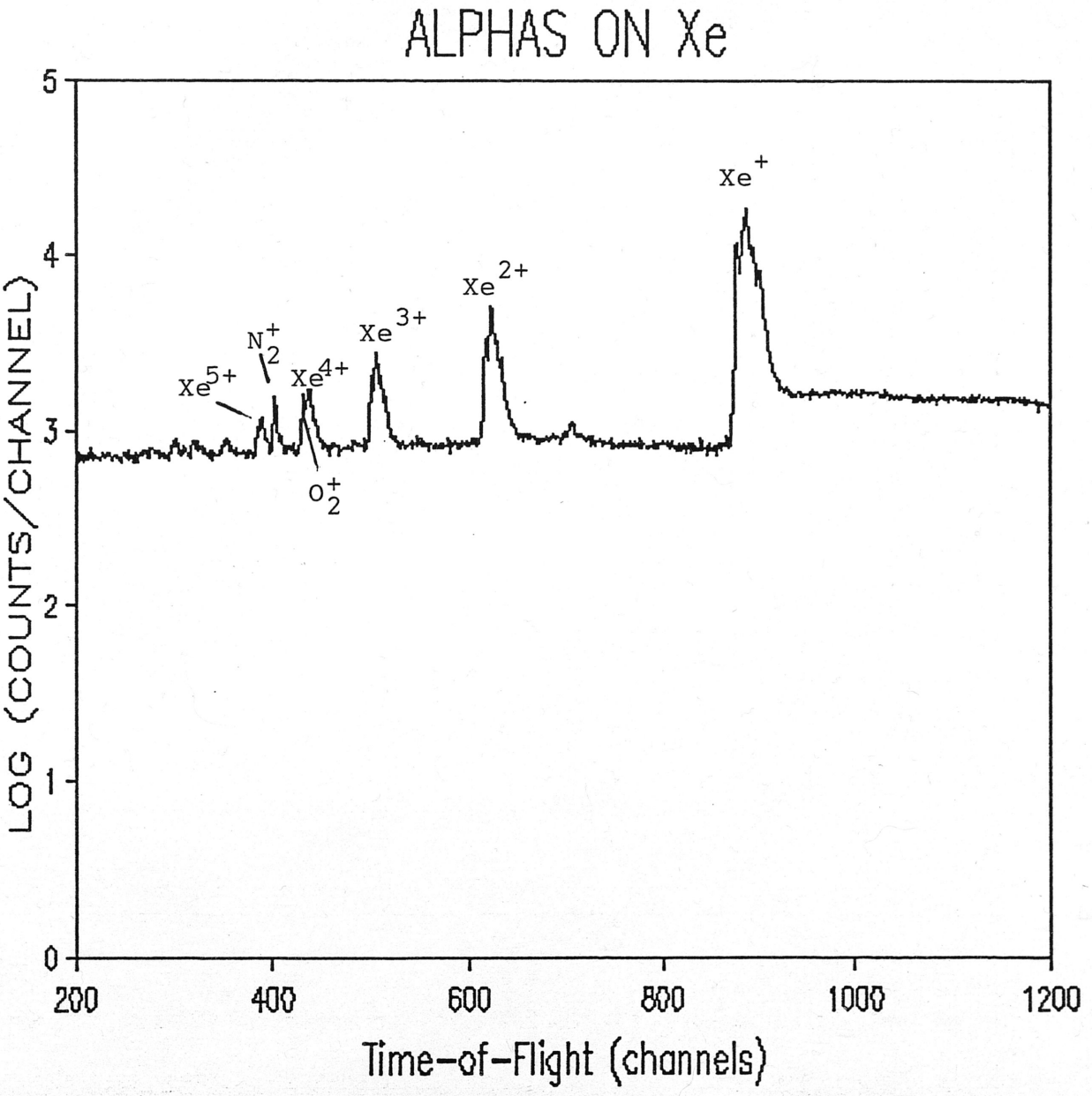

Figure 11. TOF spectrum of Xe recoil ions produced by collisions of 5.7 MeV alpha particles with Xe.

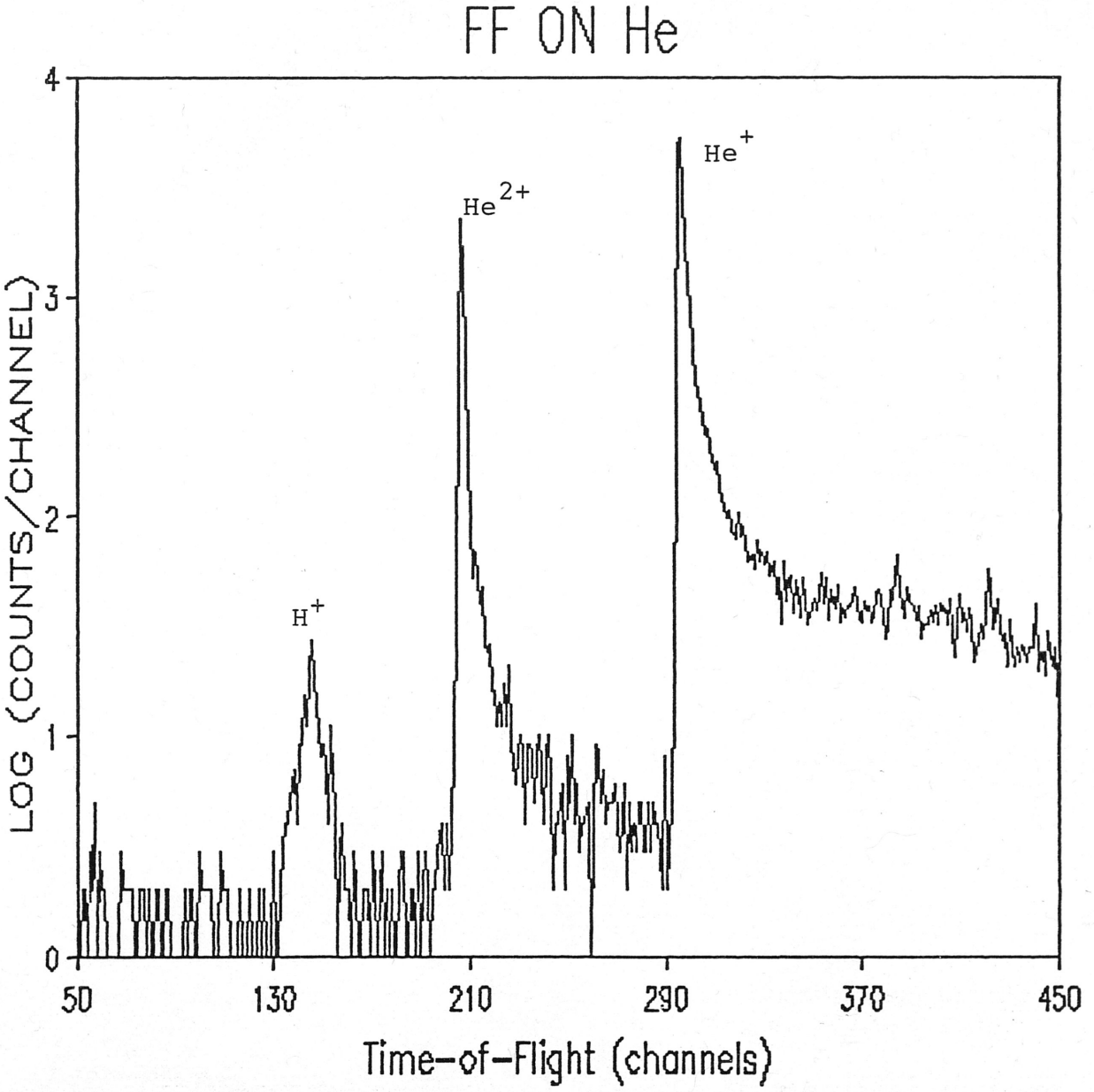

Figure 12. TOF spectrum of He recoil-ions produced by collisions of ^{252}Cf fission fragments with He.

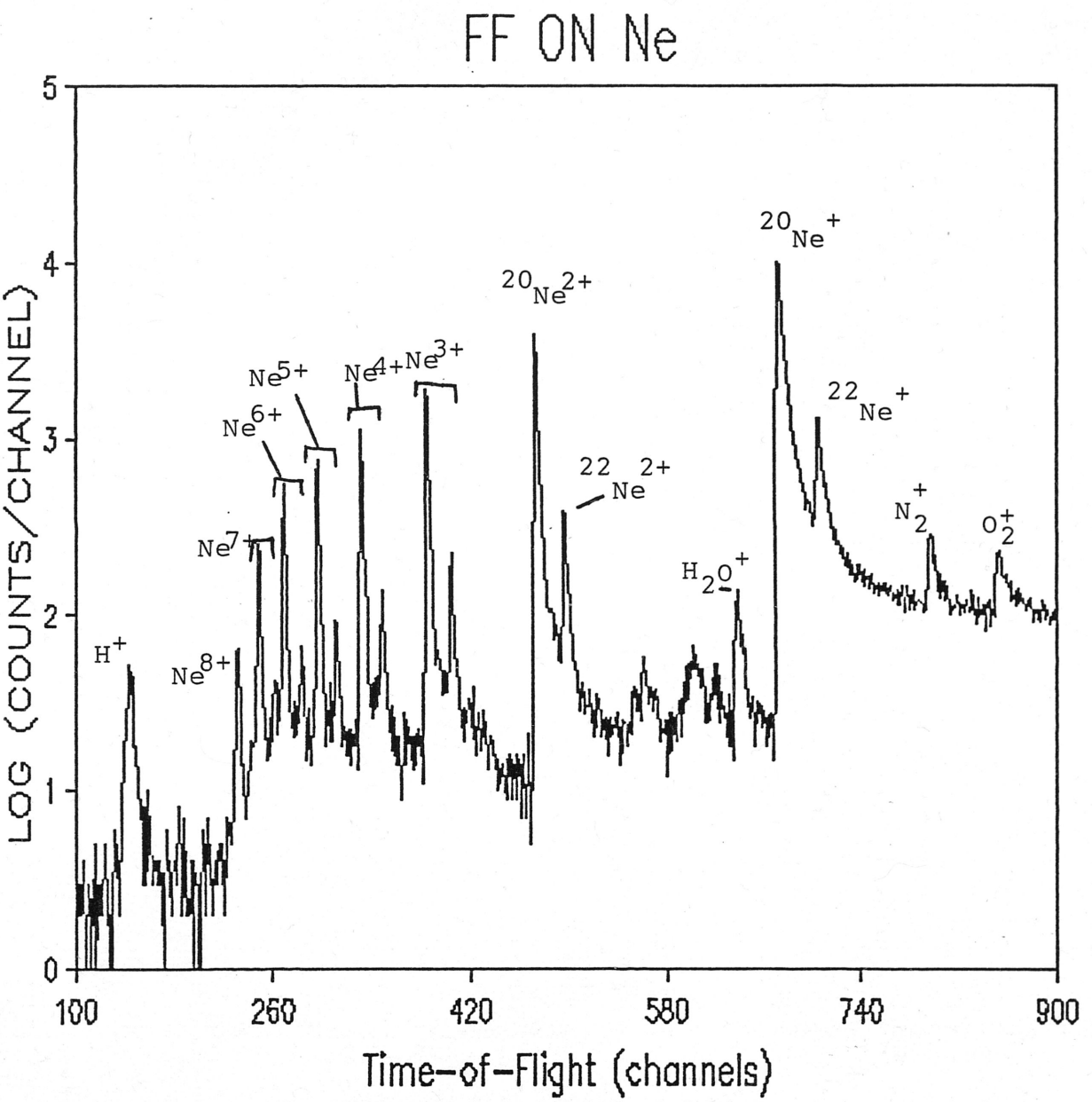

Figure 13. TOF spectrum of Ne recoil-ions produced by collisions of ^{252}Cf fission fragments with Ne.

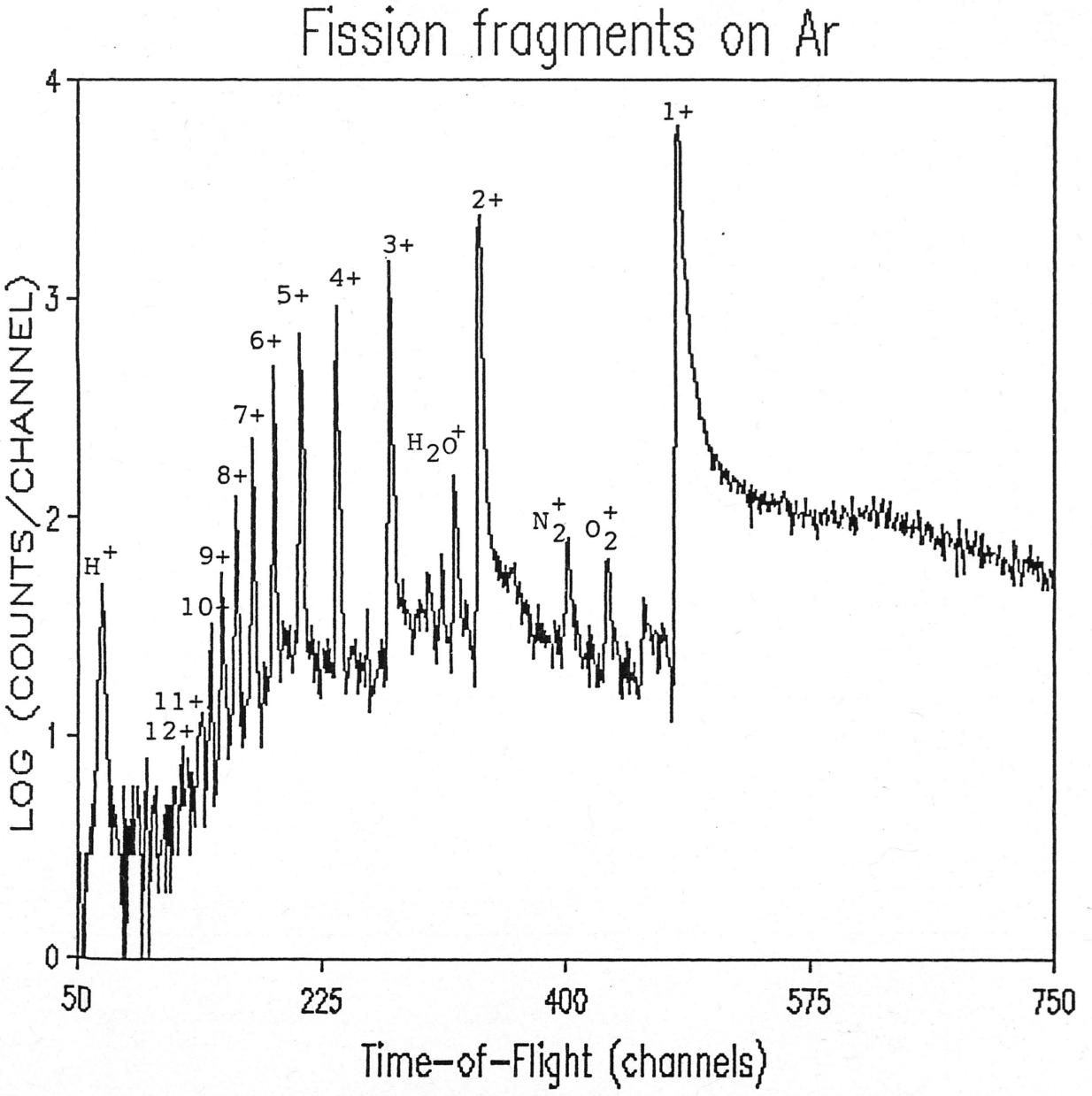

Figure 14. TOF spectrum of Ar recoil-ions produced by collisions of ^{252}Cf fission fragments with Ar.

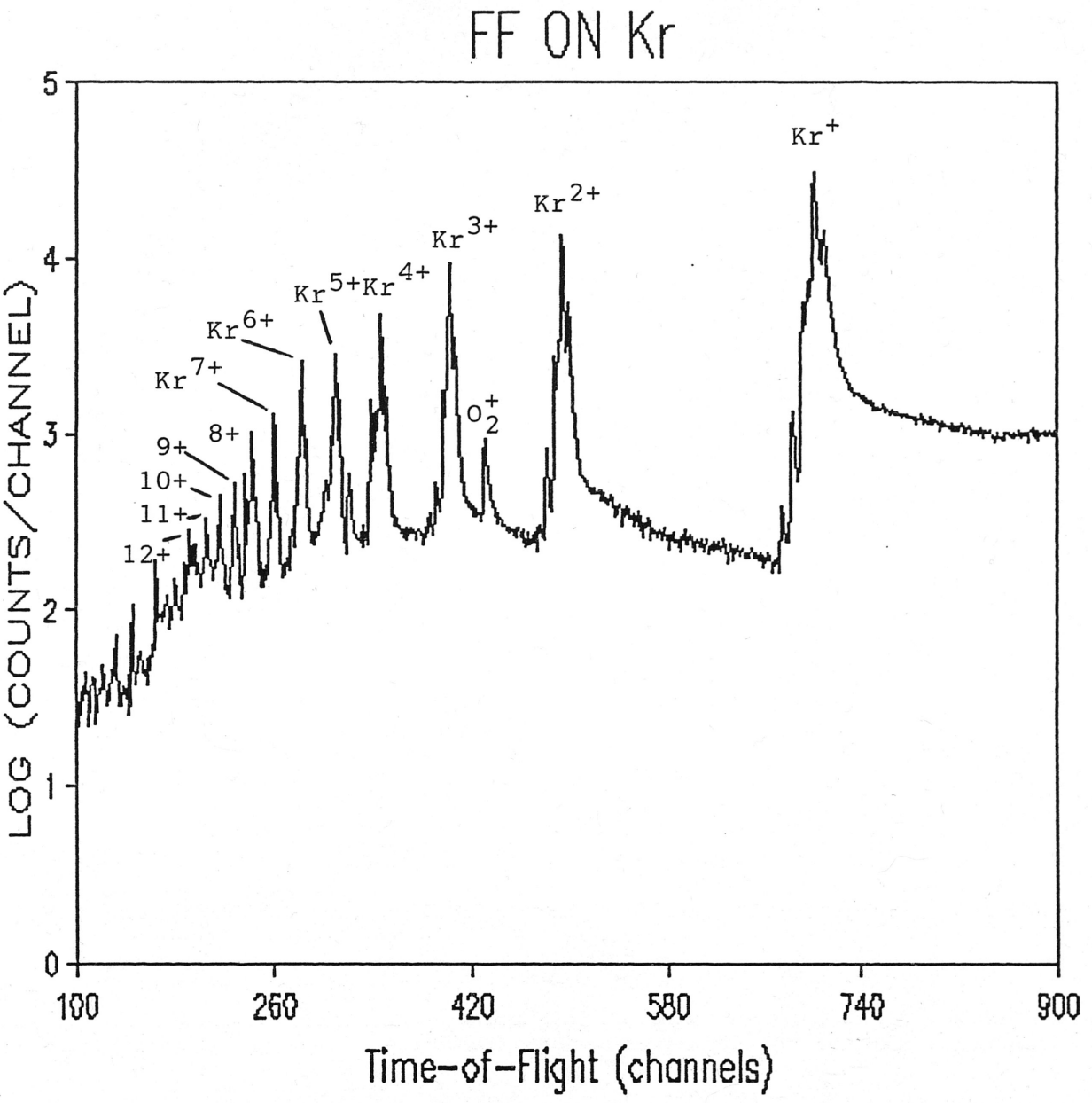

Figure 15. TOF spectrum of Kr recoil-ions produced by collisions of ^{252}Cf fission fragments with Kr.

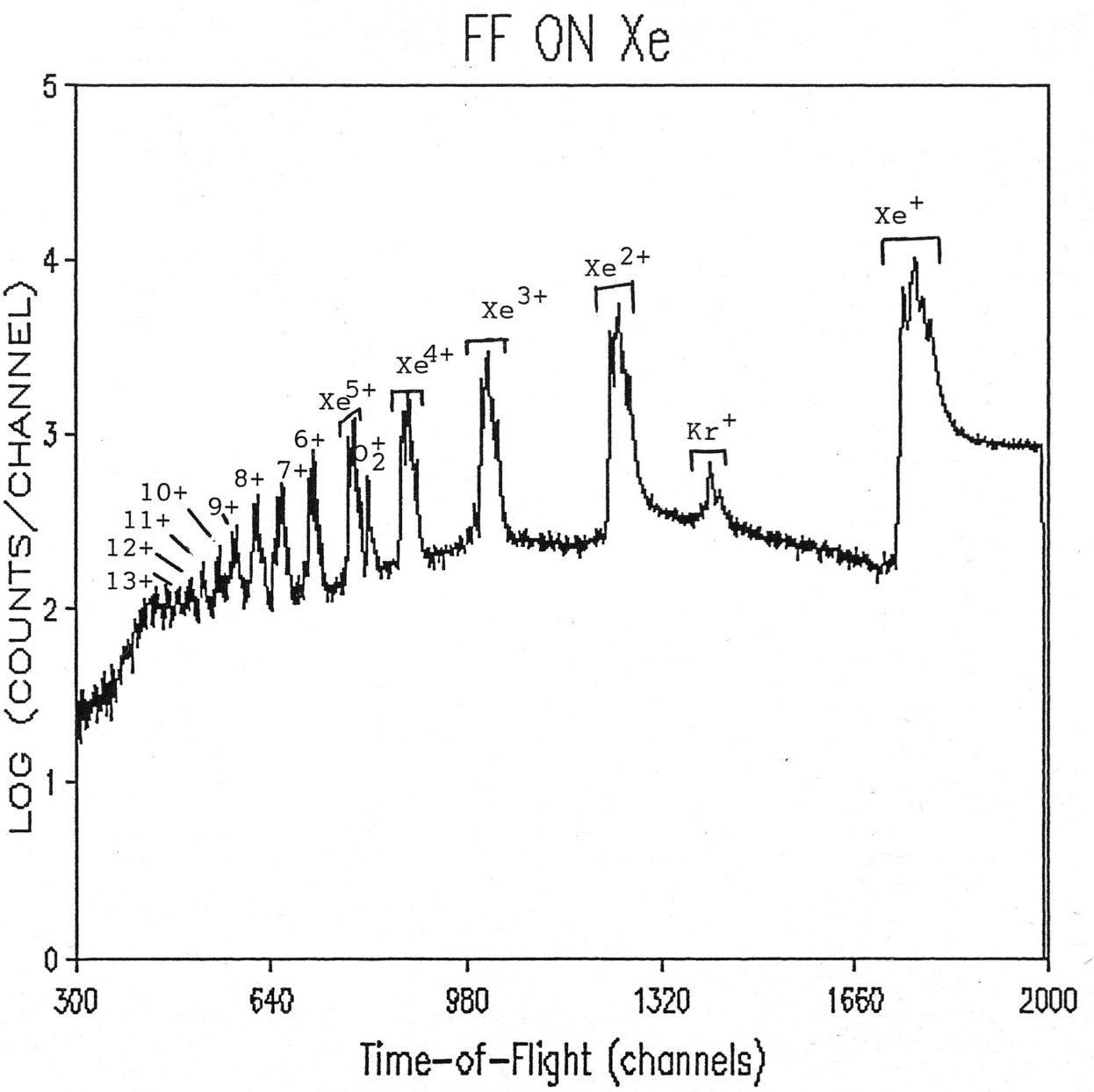

Figure 16. TOF spectrum of Xe recoil-ions produced by collisions of ^{252}Cf fission fragments with Xe.

The first step in analyzing the data was to determine the total number of incident projectiles. The alpha peak was narrower that the energy window in the TSCA, as is shown in figure 17. Thus, some lower energy alpha particles were counted, along with a few fission fragments. This caused an error in the total number of incident alpha particles recorded by the scalar and allowed some coincidence events due to projectiles other than the 5.7 MeV alpha particles to contribute to the time-of-flight spectrum. Corrections then had to be made to determine the actual number of 5.7 MeV alpha particles that were incident. Extrapolating back from the fission peak it was found that a maximum of 0.5 fission fragments per second and 1407 alpha particles per second, were allowed through the TSCA window and counted as projectiles. The incident fission fragment rate was such a small percentage of the total projectile rate, 0.036%, that this correction was deemed to be negligible compared to the other sources of experimental error. The correction for random background and the lower energy alpha particles was calculated to be approximately 2% of the true 5.7 MeV alpha particle counts. The contribution of coincidence events associated with random background and lower energy alpha particles was concluded to be negligible in light of the small percentage of counts that were not actually 5.7 MeV alpha particles. The ratio of the corrected number of 5.7 MeV alpha particles to the scalar count was used as a multiplicative correction to the scalar count to obtain the total number of alpha particles that passed through the interaction region. The energy range of the fission fragments was sufficiently broad compared to the TSCA window that every gate signal corresponded to a projectile of interest.

The scalar therefore gave an accurate count of the number of fission fragment projectiles without the need for correction.

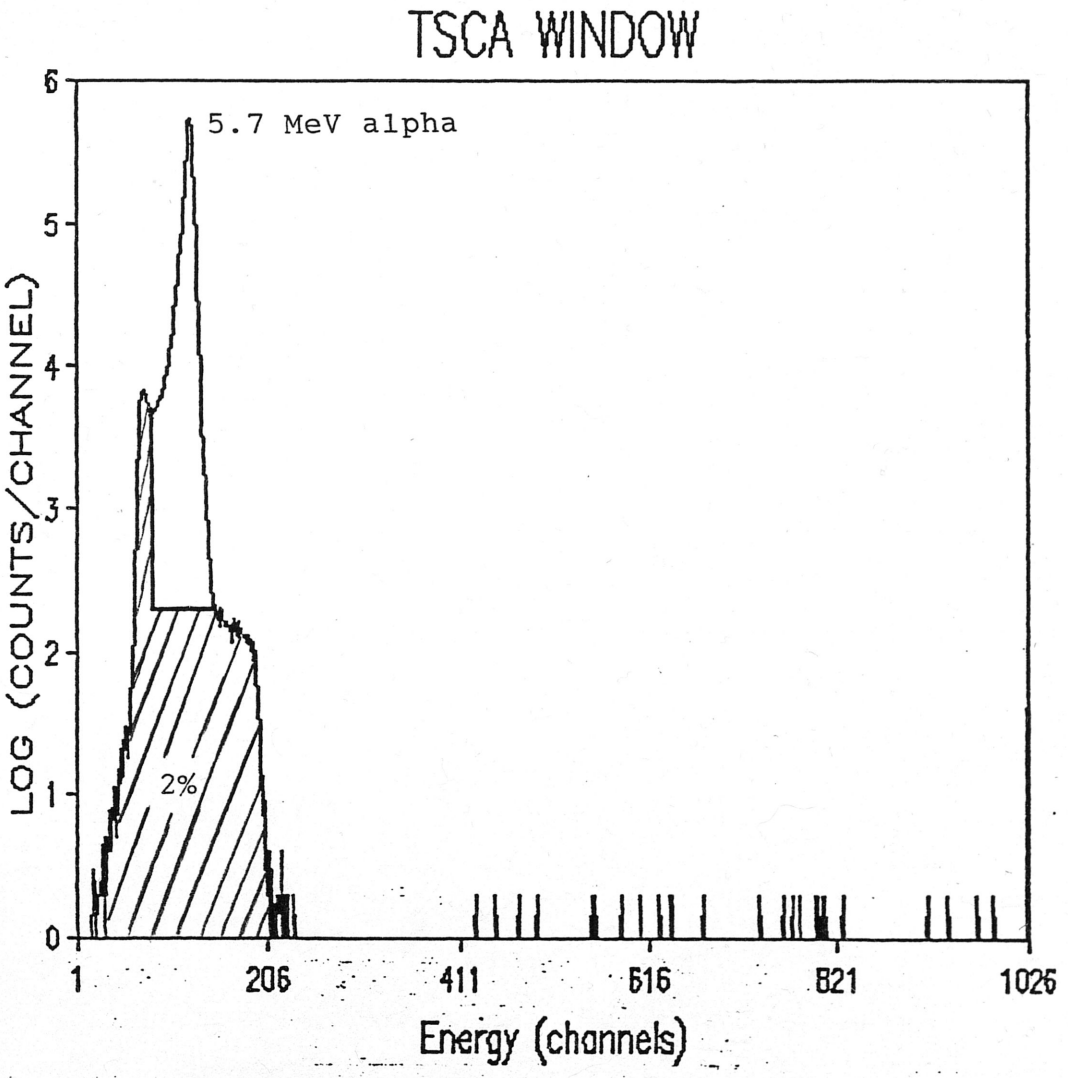

Figure 17. Si Surface Barrier Detector pulse-height spectrum of the energy range of projectiles for alpha particle measurements.

To check the pressure dependence of ion production, a series of five Ar time-of-flight spectra, each at a different pressure, were measured using fission fragments as projectiles. From these spectra, it could be verified that single collision conditions existed over the pressure range of the measurements. Single collision conditions exist when each projectile collides with no more than one target atom during its passage through the interaction region. The integrated numbers of counts, N_i, under the time peaks corresponding to the different ionic charges of the Ar recoil ions were divided by the total number of incident projectiles, N_t, and this ratio plotted versus the pressure. The results for q = 1+ to 3+ are shown in figure 18 where it is evident that the ratio N_i/N_t varies linearly with pressure. Under single collision conditions, the rate of ion production must be directly proportional to the number of target atoms, and hence to the pressure, whereas if multiple collisions occur, the rate of ion production will depend quadratically on the pressure.

Having shown that single collision conditions were fulfilled for the experiments, reliable cross sections for multielectron ionization then could be calculated from the data using the relationship

$$\sigma = [3.10\text{x}10^{-14}/(Lp\epsilon)]\ (N_i/N_t)\ \text{cm}^2, \qquad (9)$$

where

L = length of the interaction region (cm) = .274 cm

p = gas pressure (mTorr)

ϵ = total collection and detection efficiency of the recoil-ions.

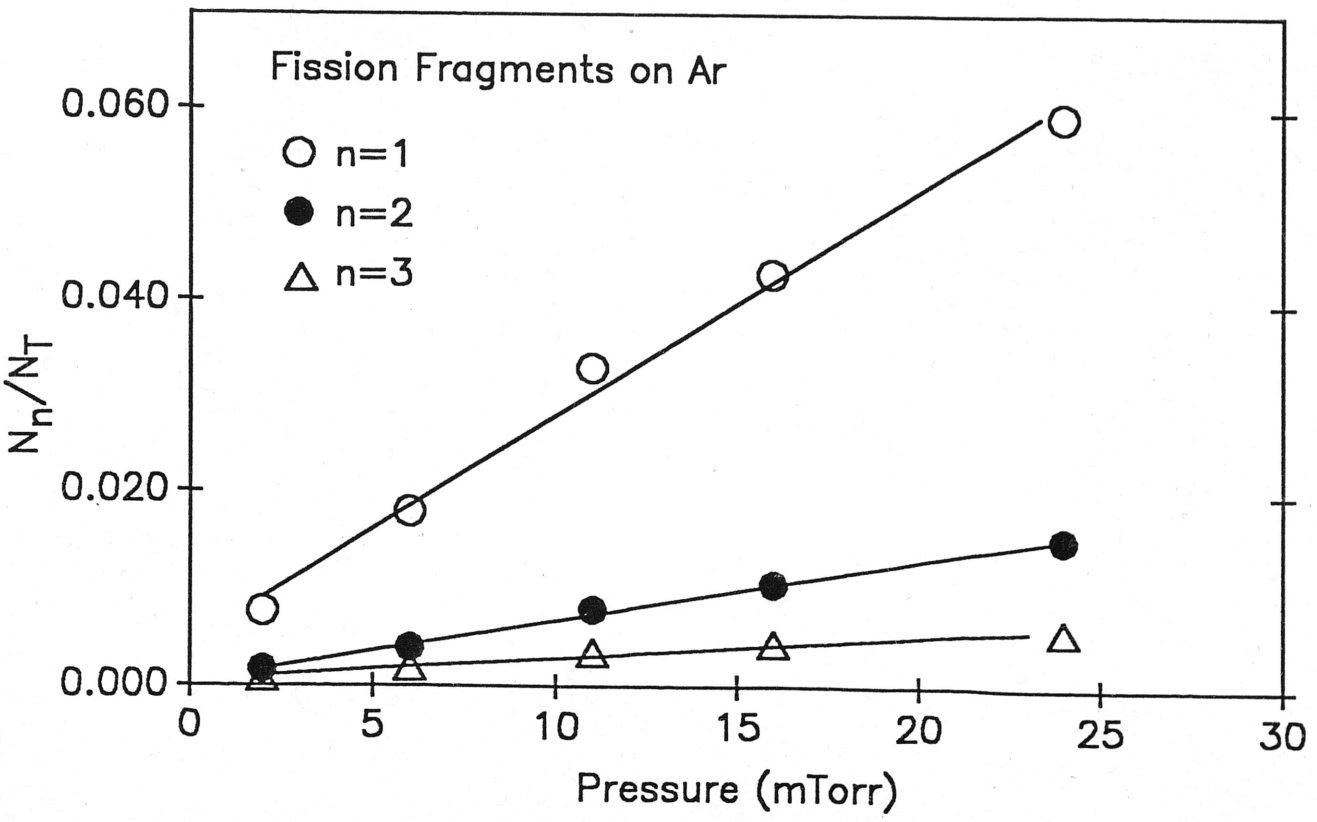

Figure 18. Pressure dependence of N_i/N_t for fission fragments colliding with Ar.

Since the pressure was measured through approximately 16 inches of .25 inch I.D. tubing (10 inches of Tygon tubing and 6 inches of copper tubing) and one valve, the measured pressure was not expected to accurately reflect the true pressure within the gas cell. The pressure in the cell should, theoretically, be higher than the measured pressure. In addition, the total ion detection and collection efficiency is very

difficult to accurately calculate. The total efficiency is the product of the transmission efficiencies through the collimator and two nickel grids on the ends of the flight tube, and the detection efficiency of the microchannel plates. Therefore, it was necessary to find a means of accurately determining the pressure-times-efficiency ($p\epsilon$) product. The K-shell ionization cross sections for alpha particles on many different elements are well known experimentally, and can be predicted very accurately by several different theoretical methods.[1,7] Using the Binary Encounter Approximation (BEA) to calculate the ionization cross section for 5.7 MeV alpha particles on He for He^{1+} production, one obtains a theoretical cross section of 4.52×10^{-17} cm^2. This cross section then was used along with the measured value of N_i/N_t to calculate the value of $p\epsilon$ for the alpha particle on He measurement. This product was scaled for different target gas pressures when converting the other measured values of N_i/N_t to ionization cross sections. Thus, using equation (8) with the value of $p\epsilon$ determined in the 5.7 MeV alpha particle on He measurement, the ionization cross sections for alpha particles and fission fragments ionizing the noble gases were obtained. Absolute errors were found using standard statistical error propagation methods, and then converted to percentages of the experimental cross sections. The ionization cross sections for alpha particles and fission fragments are given tables I and II, respectively.

Table I. Ionization cross sections for 5.7 MeV alpha particles in collision with noble gas atoms.

Ion Chg.	He	Ne	Ar	Kr	Xe
+1	4.60e-17	9.34e-17	2.05e-16	2.26e-16	2.37e-16
+2	7.89e-19	5.86e-18	1.36e-17	1.87e-17	3.89e-17
+3		5.43e-19	3.00e-18	1.19e-17	1.62e-17
+4			1.18e-18	3.12e-18	7.83e-18
+5			5.55e-19	1.26e-18	2.09e-18
+6			2.15e-19	6.15e-19	9.81e-19
+7				1.27e-19	

Cross sections for q = +1 to +4 have an average error of 10% to 15%. For q greater than +4, errors climb to a maximum of 50% for q = 7+

Table II. Ionization cross sections for 48-73 MeV, q ? +19 to +21 ^{252}Cf fission fragments in collision with noble gas atoms.

Ion Chg.	He	Ne	Ar	Kr	Xe
+1	1.61e-15	1.60e-15	4.14e-15	3.70e-15	4.28e-15
+2	4.06e-16	3.35e-16	9.71e-16	1.08e-15	1.51e-15
+3		1.49e-16	4.26e-16	5.80e-16	6.07e-16
+4		7.98e-17	2.47e-16	2.87e-16	3.23e-16
+5		5.65e-17	1.79e-16	1.82e-16	1.91e-16
+6		3.26e-17	1.12e-16	1.20e-16	9.12e-17
+7		1.68e-17	4.91e-17	5.64e-17	6.28e-17
+8		6.26e-18	3.18e-17	3.35e-17	3.90e-17
+9			1.33e-17	1.95e-17	1.78e-17
+10			8.03e-18	9.04e-18	8.91e-18
+11			1.74e-18	5.01e-18	8.53e-18
+12				2.50e-18	

Cross sections for q = 1+ to 6+ have an average error of 10%. For q = 7+ to 12+, errors range from 15% to 35%.

V. DISCUSSION

The cross sections for ionization of noble gas atoms by alpha particles and fission fragments are displayed as a function of ionic charge, n, in figures 19 and 20, respectively. The most obvious characteristic of the cross sections is the large increase in magnitude in going from alpha particles to fission fragments. A theoretical description of the collision process employing the plane wave born approximation (PWBA) predicts that for single ionization, the ionization cross section should vary as the square of the projectile charge.[12] The square of the ratio of the average fission fragment charge to the alpha particle charge is approximately 100. The experimental ratio for single ionization, however, is much smaller than this, as is shown in figure 21. This discrepancy is made worse by the fact that the alpha particles have much higher velocities than the fission fragments. When this velocity difference is taken into account, theory predicts the ratio of cross sections should be approximately 290. The dependence of the ionization cross sections on target atomic number is largely determined by the electron binding energies. The binary encounter approximation (BEA) predicts that the cross sections should vary as the reciprocal of the binding energy squared. A comparison of the experimental cross sections for single ionization by 5.7 MeV alpha particles with those calculated using the BEA is shown in figure 22. The overall trend of the cross sections is correctly predicted by the BEA, but the experimental cross sections increase more slowly with atomic number than do the theoretical cross sections.

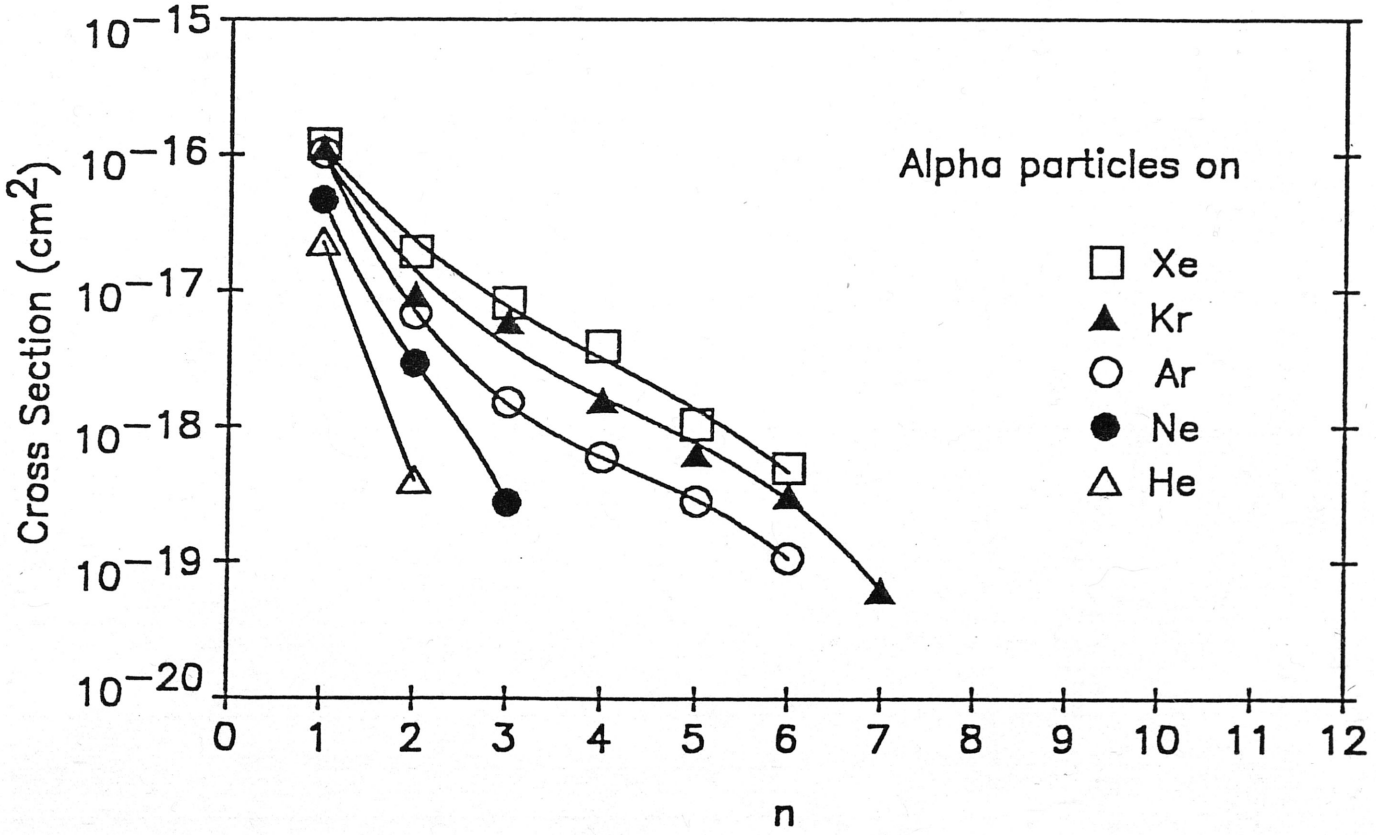

Figure 19. Ionization cross sections for 5.7 MeV alpha particles in collision with noble gas atoms.

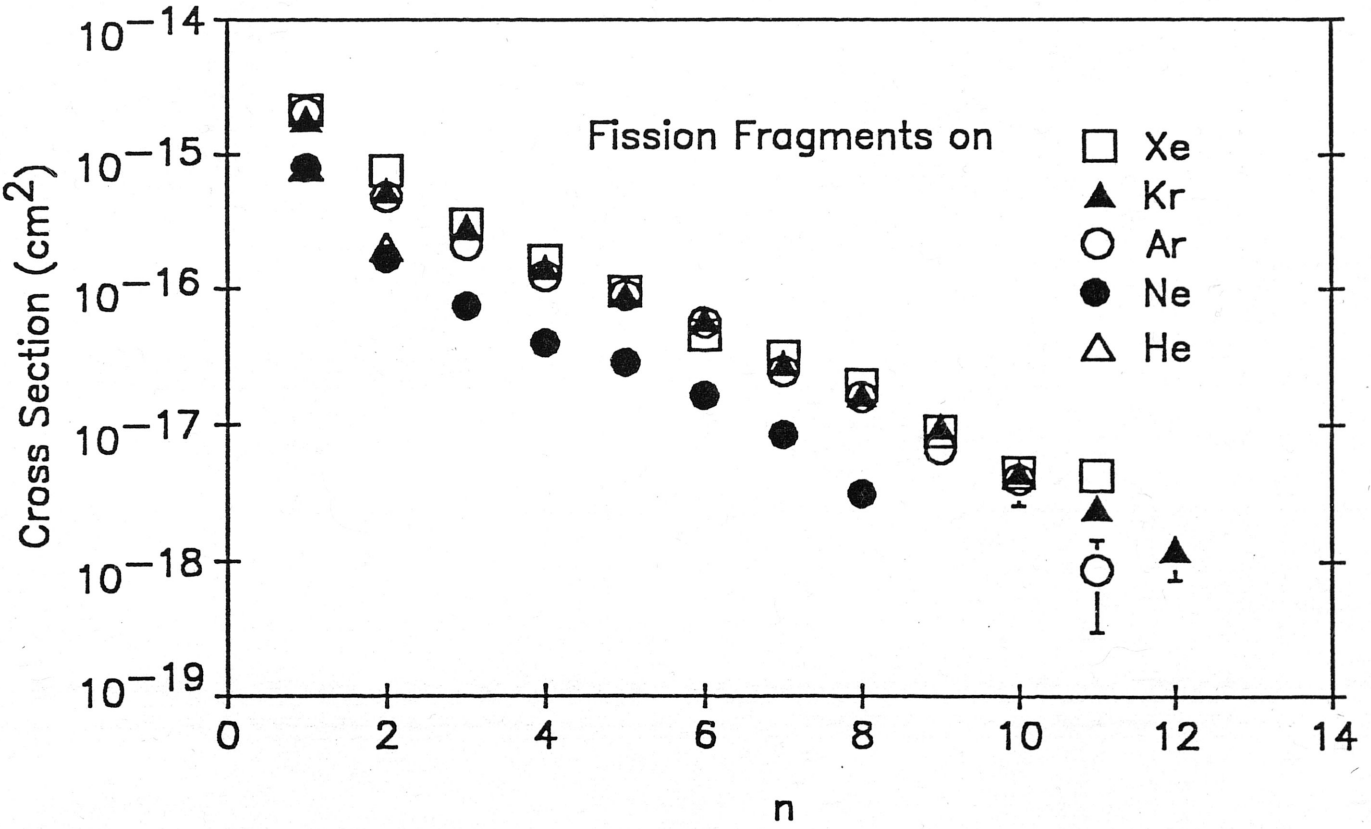

Figure 20. Ionization cross sections for 48-73 MeV, $q \approx +19$ to $+21$ ^{252}Cf fission fragments in collision with noble gas atoms.

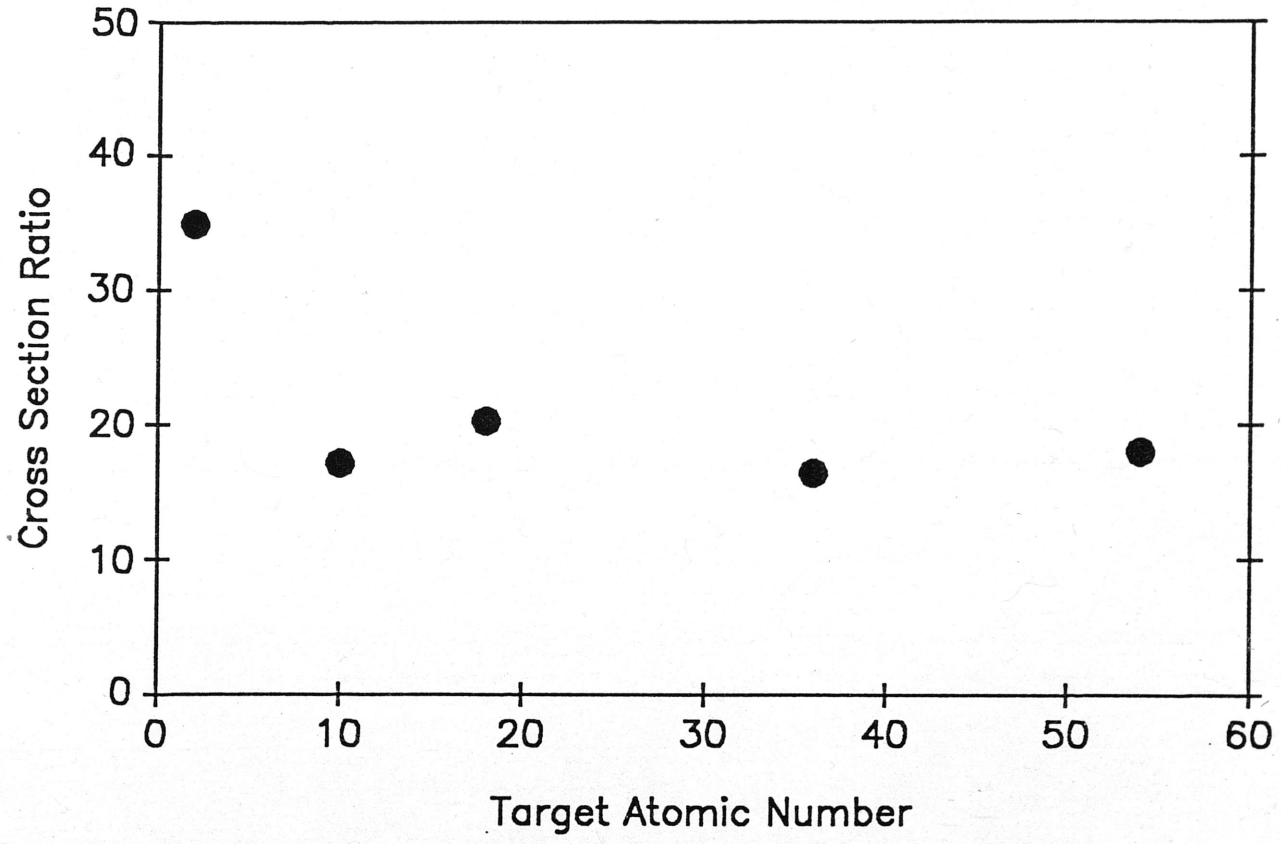

Figure 21. Single ionization cross section ratios of fission fragments to 5.7 MeV alpha particles in collision with noble gas atoms.

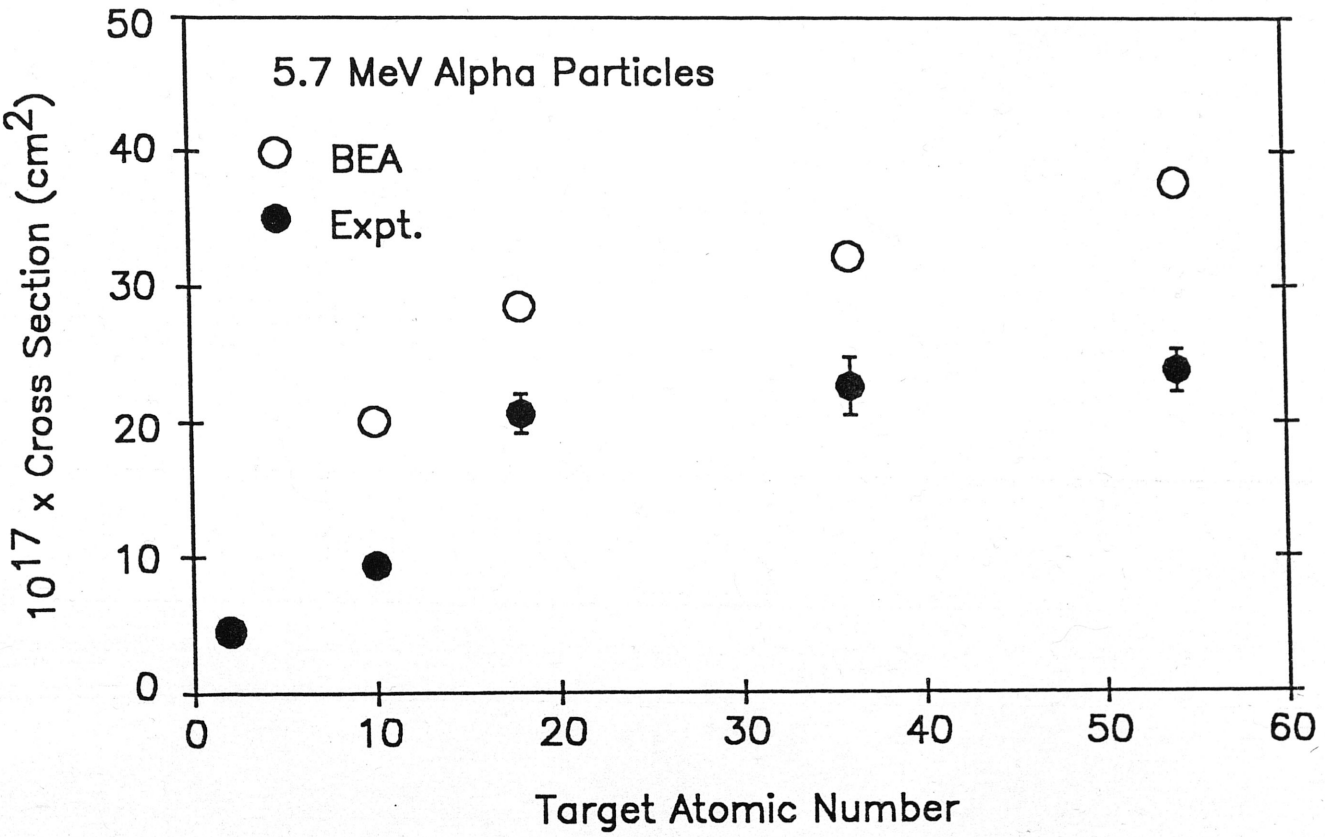

Figure 22. BEA predicted cross sections compared to experimentally measured cross sections for 1+ ionization of noble gas atoms in collision with 5.7 MeV alpha particles.

Referring back to figure 20, it may be seen that the data for fission fragments shows a grouping of the cross sections into two distinct sets (AR-Kr-Xe and He-Ne). The BEA results shown in figure 22 do in fact predict the Ar-Kr-Xe grouping, but not the He-Ne grouping.

The data also shows that the fission fragments can produce much higher recoil-ion charge states than the alpha particles. These higher charge states ($q \geq 4+$), as stated earlier, are hypothesized to result from electron capture of inner-shell target electrons into the projectile orbits.[8] The probability of capturing electrons from the target atoms by the projectiles is highest when the ratio of the projectile velocity to the target electron velocity is nearly one. The ratio of the fission fragment velocities to the target electron velocities in the Ne-K, Ar-L, Kr-M, and Xe-M shells, are approximately one, as shown in figure 23.

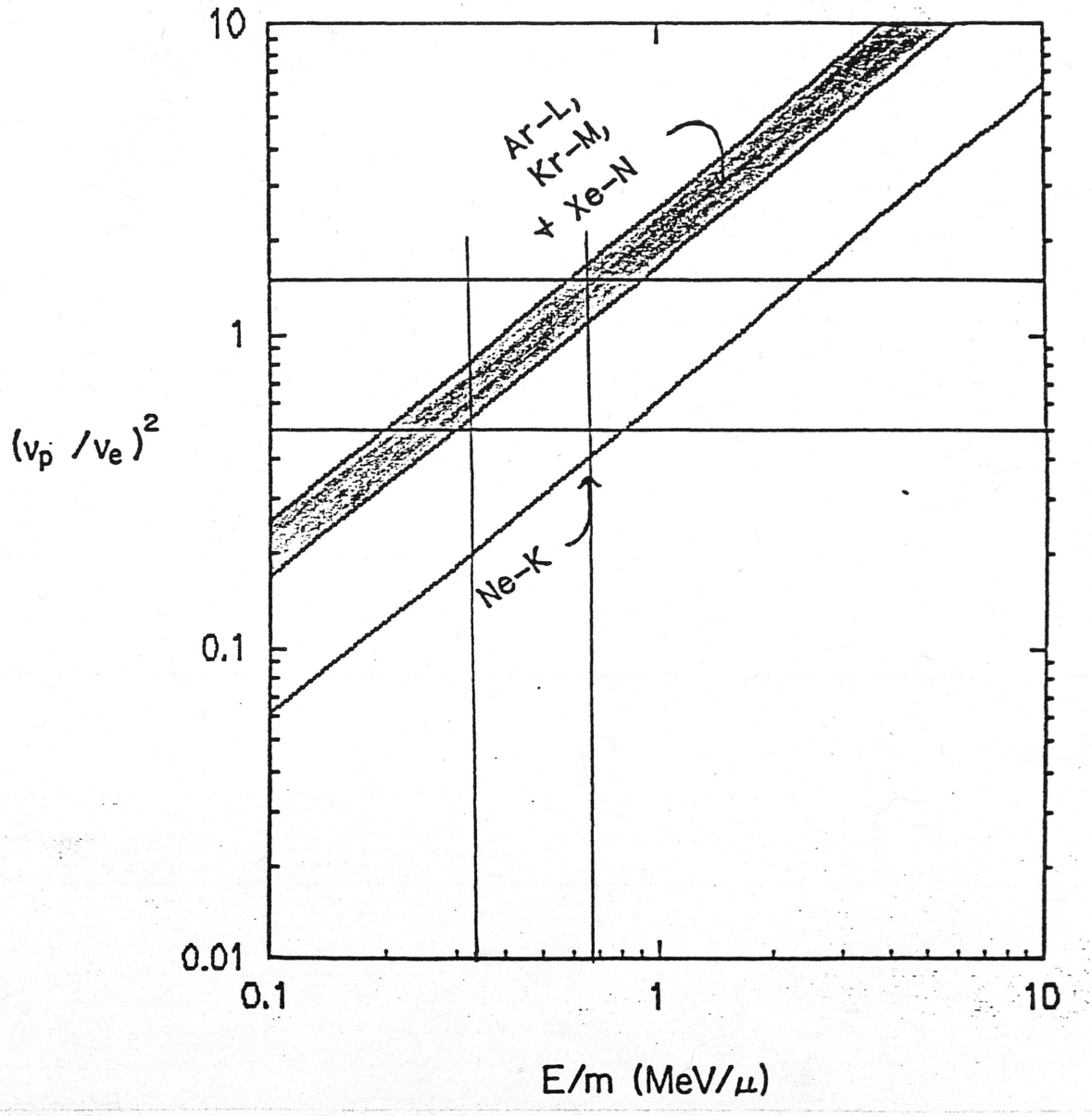

Figure 23. The square of the projectile velocity to electron velocity ratio versus the energy to mass ratio (MeV/amu) of the projectile. The two vertical lines indicate the energy to mass ratios of the two most probable ^{252}Cf fission fragments.

VI. CONCLUSIONS

Three main conclusions can be drawn from this work A) The fission fragments of ^{252}Cf provide a simple and convenient method for creating highly ionized atoms and molecules for direct study or for use in other experiments, B) Interesting discrepancies were found between the measured cross sections for single ionization and those preicted by simple theoretical descriptions, C) The cross sections measured for multielectron ionization provide a challenging new body of data for testing and stimulating new theoretical developments.

REFERENCES

1. G. Friedlander, J. W. Kennedy, E. S. Macias, and J. M. Miller. *Nuclear and Radiochemistry*, John Wiley & Sons: New York, 1981.

2. C. L. Cocke, Phys. Rev. A 20, No. 3, 749 (1979).

3. C. L. Cocke, R. DuBois, T. J. Gray, E. Justiniano, C. Can, Phys. Rev. Lett. 46, 1671 (1981).

4. C. R. Vane, M. H. Prior, and R. Marrus, Phys. Rev. Lett. 46, 107 (1981).

5. C. Schmeissner, C. L. Cocke, R. Mann, and W. Meyerhof, Phys. Rev. A 30, 1661 (1984).

6. P. Richard, J. Ullrich, S. Kelbch, H. Schmidt-Bocking, R. Mann, and C. L. Cocke, Nucl. Inst. and Meth. A 240, 532 (1985).

7. R. J. Maurer, *Ionization and Fragmentation of Molecular Gases In Collisions with MeV/amu Heavy Ions*, Dissertation, Texas A&M University, May 1988.

8. O. Heber, G. Sampoll, R. J. Maurer, B. B. Bandong, and R. L. Watson, Nucl. Inst. and Meth. B 41, 197 (1989).

9. R. L. Watson, *A Study of the Internal Conversion Electrons Emitted Within Three Nanoseconds After the Spontaneous Fission of* ^{252}Cf, Ph. D. Thesis, University of California at Berkeley, July 1966.

10. D. A. Dahl and J. E. Delmore, SIMION PC/AT User's Manual Version, EG&G Idaho National Engineering Laboratory (1986).

11. W. C. Wiley and I. H. McLaren, Rev. Sci. Instr. 26, 1150 (1955).

12. H. Bethe, Ann. Phys. 5, 325 (1930).